Spacecraft Attitude Estimations Using Phase Information of GPS Signals

S. Purivigraipong

Department of Electronic Engineering, Mahanakorn University of Technology
Phone (662) 988 3655, Fax (662) 988 4040, e-mail: sompop@mut.ac.th

Abstract

This paper presents an implementation of an EKF (extended Kalman filtering) estimator for spacecraft attitude determination using GPS (Global Positioning System) signals. The spacecraft dynamics under small rotation angles is modelled using Euler angles (roll, pitch and yaw) parameterisations which are applicable for real-time operation onboard spacecraft. The torque from the Earth's gravitation field and magnetorquers is modelled in order to cope with perturbations. The filtering estimator is tested with simulated GPS data, and flight GPS data collected from the real spacecraft. The results shows that the estimated attitude derived from both simulated and flight data were in agreement with the reference attitude. A contribution from this paper is that the analytical formulation identifies two state vectors that keep the pitch state independent of roll and yaw. This results in significantly reducing the dimensions of computation.

Keywords: Kalman filtering, spacecraft attitude, GPS.

1. Introduction

In the traditional way, spacecraft attitude determination depends upon attitude sensors, such as magnetometers, Sun sensors, Earth sensors, inertial measurement units (IMU), and star sensors. The selection of attitude sensor basically depends upon the required pointing mode of the mission (e.g. inertial pointing or Earth pointing), accuracy requirement, power consumption budget, and cost [1].

However, since the use of Global Positioning Systems (GPS) has been successfully demonstrated in space navigation [2], a new approach is now available using GPS for attitude determination which is potentially attractive for spacecraft applications [3]. The benefits of using a GPS receiver with multiple antennas can be explained by comparing the new attitude sensor and typical attitude sensors in three aspects.

Measurement Availability: The tracking data from PoSat's GPS receiver showed that four or more GPS satellites can be seen for 80% of the time in low Earth orbit [4]. Improvement over this has been demonstrated with the next generation of GPS receivers. This suggests that a GPS attitude sensor can provide almost continuous measurements (whereas the Sun sensor cannot provide data in eclipse period).

Orbit/Attitude Determination Unit: A GPS receiver with multiple antennas for spacecraft navigation generally provides position, software needs to include carrier phase measurement and attitude estimation sub-routines. Then, the GPS receiver can be used for both orbit and attitude determination.

A part of the content has appeared and been discussed at the 25th Electrical Engineering Conference (EECON-25) on 21-22 Nov. 2002 held at Prince of Songkla University, Hat Yai, Songkla, Thailand.

Cost and Power Budget: Currently, GPS technology is rapidly developing in order to reduce the size, weight, power consumption and cost. This should make the GPS receiver even more attractive for spacecraft missions. As part of this trend, NASA plans to use GPS receivers on all its spacecraft to demonstrate both orbit and attitude experiment [5].

In earlier times, the spacecraft attitude was traditionally derived from the deterministic algorithms such as QUEST (quaternion estimator) [6] and TRIAD [7]. However, a new approach to linear filtering, namely "Kalman filter, was proposed in 1960 [8]. Kalman filtering has recently been used widely for spacecraft attitude estimation [9]. Unlike the deterministic algorithms, the Kalman filter uses dynamic and/or kinematic models, and estimates spacecraft attitude using a time series of measurements.

Over recent years, Kalman filters have been widely used for GPS attitude determination. A Kalman filter based on quaternion parameters was presented in [10]. The filter was implemented for single and dual antenna baseline. The simulated results showed that the dual baseline provided a robust solution. The advantage of the quaternion-based model was that the model copes with the condition of large angle manoeuvres. However, the dimension of computation and computer burden may be impractical for real operation.

In this paper, the implemented filtering estimator based on Euler-angle parameters offers the analytical formulation which identifies two state vectors that keep the pitch state independent of roll and yaw. Therefore, an original (6×6) covariance matrix can be replaced with the (4×4) and (2×2) matrices. This results in significantly reducing the dimensions of computation. Furthermore, the analytic formulation of process noise was much simply compared to the quaternion-based model.

2. Background

2.1 GPS Attitude Measurement

The observable in GPS attitude sensing is the carrier path difference, r (in length unit), between two antennas separated by the baseline length, l. For each GPS antenna, the received carrier phase signal is measured at the apparent phase centre of the antenna itself. A relative phase difference between the received signals from two antennas is defined as carrier phase difference, φ (radian unit). If the length of baseline vector, l, is larger than one carrier wavelength of the GPS L1 frequency, the number of full cycles is unknown.

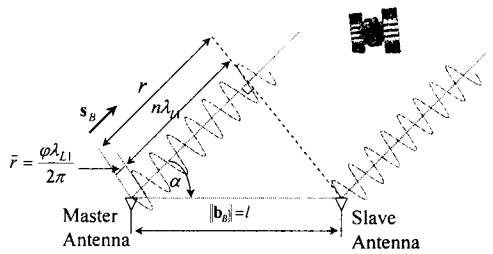

Figure 1. Carrier path difference for GPS attitude sensing

The mechanism of GPS attitude sensing can be explained from geometry as shown in Figure 1. A projection of the baseline vector on the line of sight vector to the GPS satellite is defined as *single path difference*, r (in length unit).

$$r = \frac{\varphi\lambda_{L1}}{2\pi} + n\lambda_{L1} \equiv \bar{r} + n\lambda_{L1} \qquad (1)$$

where n is an *unknown* integer cycle, λ_{L1} is a carrier wavelength of the GPS L1 frequency (1.57542 GHz), and $\bar{r}$ is a modulo path difference.

The path difference r in Equation (1) can also be expressed in a vector dot product form which shows an attitude transformation matrix, **A**,

$$r = (\mathbf{s}_B \cdot \mathbf{b}_B) = \mathbf{b}_B^T \mathbf{A} \mathbf{s}_O \qquad (2)$$

where $\mathbf{s}_O$ is a *known* unit vector directed to GPS satellite in orbit-defined frames, $\mathbf{b}_B$ is a *known* baseline vector in the body coordinate frame.

2.2 Euler Angles Parameterisation

The orientation of spacecraft may be defined by three angles (roll, pitch, and yaw). These angles are obtained from the sequence of right hand positive rotation from a ($\mathbf{X}_R$, $\mathbf{Y}_R$, $\mathbf{Z}_R$) set of reference axes to a ($\mathbf{X}_B$, $\mathbf{Y}_B$, $\mathbf{Z}_B$) set of body-fixed axes. Therefore, there are 12 possible sequences of rotation, which can be expressed with Euler angles. One example is a 2-1-3 rotation as shown in Figure 2. The first rotation is a pitch about the $\mathbf{Y}_O$ axis, which defines a pitch angle (θ). The second rotation is a roll about the intermediate **L** axis, and defines a roll angle (ϕ). The last rotation is a yaw about the $\mathbf{Z}_B$ axis, defining a yaw angle (ψ).

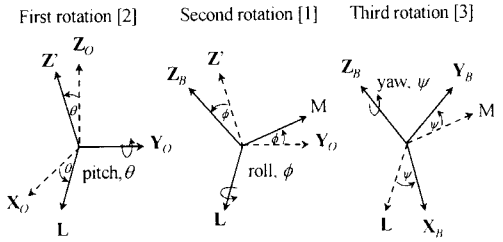

Figure 2. Euler angle type 2-1-3 interpretation

The attitude matrix computed from Euler angles for 2-1-3 system, **A**, which transforms an arbitrary vector from the orbit-defined coordinates to spacecraft body-fixed coordinates can be expressed as [7]

$$\mathbf{A} = \begin{bmatrix} c\psi c\theta + s\psi s\phi s\theta & s\psi c\phi & -c\psi s\theta + s\psi s\phi c\theta \\ -s\psi c\theta + c\psi s\phi s\theta & c\psi c\phi & s\psi s\theta + c\psi s\phi c\theta \\ c\phi s\theta & -s\phi & c\phi c\theta \end{bmatrix} \tag{3}$$

where c is a cosine function, and s is a sine function.

The roll, pitch and yaw attitude angles of 2-1-3 sequential rotation system can be calculated from

$$\begin{aligned} \text{roll}(\phi) &= \sin^{-1}(-a_{32}) \\ \text{pitch}(\theta) &= \tan^{-1}(a_{31}/a_{33}) \\ \text{yaw}(\psi) &= \tan^{-1}(a_{12}/a_{22}) \end{aligned} \tag{4}$$

where a_{ij} is an element of the attitude matrix.

2.3 Attitude Dynamics

It is supposed that a rigid body is moving in inertial coordinates. The motion can be described by the translation motion of its centre of mass, together with a rotation motion of the body about some axis through its centre of mass. The rotation motion is caused by the applied moment. The basic equation of attitude dynamics relates the time derivative of the angular momentum vector.

In the case of spacecraft equipped with fixed-wheels, it is no longer a rigid body. Including the influence of the gravity gradient, magnetic firing, and reaction wheel angular momentum, the dynamic equations in body-fixed coordinates can be expressed as [7]

$$\mathbf{I}_{MOI}\dot{\boldsymbol{\omega}}_B^I = (\mathbf{N}_G + \mathbf{N}_M) - \boldsymbol{\omega}_B^I(\mathbf{I}_{MOI}\boldsymbol{\omega}_B^I + \mathbf{h}_W) - \dot{\mathbf{h}}_W \tag{5}$$

where $\mathbf{N}_G$ is a gravity-gradient torque vector,

$\mathbf{N}_M$ is a torque vector generated by magnetorquers

$\mathbf{I}_{MOI}$ is a moment of inertia tensor of spacecraft,

$$\mathbf{I}_{MOI} = \begin{bmatrix} I_{xx} & -I_{xy} & -I_{xz} \\ -I_{yx} & I_{yy} & -I_{yz} \\ -I_{zx} & -I_{zy} & I_{zz} \end{bmatrix} \tag{6}$$

$\boldsymbol{\omega}_B^I$ is an angular rate vector referenced to the inertial frame, expressed in body-fixed coordinates,

$\mathbf{h}_W$ is a relative wheel angular momentum vector,

$\dot{\mathbf{h}}_W$ is wheel torque vector.

3. Simplified Model of Earth-Pointing Spacecraft Dynamics under Small Rotation Angles

This section describes spacecraft dynamics under small rotation angles using Euler angle representation. The Earth-pointing spacecraft is widely used for communication satellites and Earth observation satellites. The spacecraft rotates at one revolution per orbit in a near

circular orbit with orbital angular rate, ω_o. The orbital rate vector can be written as

$$\boldsymbol{\omega}_o = \begin{bmatrix} 0 & -\omega_o & 0 \end{bmatrix}^T \quad (7)$$

The attitude angles are defined as roll, pitch and yaw which are treated as small errors about the velocity vector. The transformation matrix (for 2-1-3 system) from orbit-defined coordinates to the body-fixed coordinates can be expressed as

$$\mathbf{A} \cong \begin{bmatrix} 1 & \psi & -\theta \\ -\psi & 1 & \phi \\ \theta & -\phi & 1 \end{bmatrix} \quad (8)$$

The body angular rate vector referenced to orbit-defined coordinates can be derived from the rate of change of Euler angles (2-1-3)

$$\boldsymbol{\omega}_B^O = \begin{bmatrix} \omega_{Ox} & \omega_{Oy} & \omega_{Oz} \end{bmatrix}^T \cong \begin{bmatrix} \dot{\phi} & \dot{\theta} & \dot{\psi} \end{bmatrix}^T \quad (9)$$

where $\boldsymbol{\omega}_B^O$ is an angular rate vector referenced to the orbit-defined frame, expressed in body-fixed coordinates.

The body angular velocity vector referenced to inertial coordinate system can be derived

$$\boldsymbol{\omega}_B^I = \boldsymbol{\omega}_B^O + \mathbf{A}\boldsymbol{\omega}_o \equiv \begin{bmatrix} \dot{\phi} \\ \dot{\theta} \\ \dot{\psi} \end{bmatrix} + \mathbf{A}\begin{bmatrix} 0 \\ -\omega_o \\ 0 \end{bmatrix} = \begin{bmatrix} \dot{\phi} - \omega_o\psi \\ \dot{\theta} - \omega_o \\ \dot{\psi} + \omega_o\phi \end{bmatrix} \quad (10)$$

where $\omega_o^2 = \mu_\oplus / \mathbf{R}_S^3$ is the orbital angular velocity of the spacecraft in the circular orbit of radius $\mathbf{R}_S^3$, and $\mu_\oplus$ is the Earth's gravitational constant. For example a typical orbit of a microsatellite at 800 km altitude is ω_o = 0.059 degree/second.

The zenith vector along the yaw axis in the orbit-defined coordinates is $\begin{bmatrix} 0 & 0 & -1 \end{bmatrix}^T$. Thus, the zenith vector in the body-fixed coordinates system, $\vec{\mathbf{z}}_B$, is

$$\vec{\mathbf{z}}_B = \mathbf{A}\begin{bmatrix} 0 & 0 & -1 \end{bmatrix}^T = \begin{bmatrix} \theta & -\phi & -1 \end{bmatrix}^T \quad (11)$$

The simplified formulation of gravity-gradient torque, $\mathbf{N}_G$, on the entire spacecraft can be expressed [7]

$$\mathbf{N}_G = 3\omega_o^2 \vec{\mathbf{z}}_B \times (\mathbf{I}_{MOI}\vec{\mathbf{z}}_B) \equiv 3\omega_o^2 \begin{bmatrix} (I_{zz} - I_{yy})\phi \\ (I_{zz} - I_{xx})\theta \\ 0 \end{bmatrix} \quad (12)$$

The above equation is simplified by linearisation for a spacecraft in a near circular orbit using small-angle approximation for ϕ and θ.

If we consider only the torque from Earth's gravitational field, the dynamic equation in the body-fixed coordinates system can be expressed as

$$\mathbf{I}_{MOI}\dot{\boldsymbol{\omega}}_B^I = \begin{bmatrix} 3\omega_o^2(I_{zz} - I_{yy})\phi - (I_{zz} - I_{yy})\omega_y\omega_z \\ 3\omega_o^2(I_{zz} - I_{xx})\theta + (I_{zz} - I_{xx})\omega_x\omega_z \\ (I_{xx} - I_{yy})\omega_x\omega_y \end{bmatrix} \quad (13)$$

where $\boldsymbol{\omega}_B^I = \begin{bmatrix} \omega_x & \omega_y & \omega_z \end{bmatrix}^T$.

If the satellite has a symmetric structure in the x and y axes ($I_{xx} = I_{yy} = I_t$ = transverse inertia momentum), the dynamics equations are then rewritten as

$$\mathbf{I}_{MOI}\dot{\boldsymbol{\omega}}_B^I \approx \begin{bmatrix} 3\omega_o^2(I_{zz} - I_t)\phi - (I_{zz} - I_t)\omega_z\omega_y \\ 3\omega_o^2(I_{zz} - I_t)\theta + (I_{zz} - I_t)\omega_z\omega_x \\ 0 \end{bmatrix} \quad (14)$$

From Equation (10), the first-order derivative of the body-fixed angular rate vector is

$$\dot{\boldsymbol{\omega}}_B^I = \begin{bmatrix} (\ddot{\phi} - \omega_o\dot{\psi}) & \ddot{\theta} & (\ddot{\psi} + \omega_o\dot{\phi}) \end{bmatrix}^T \quad (15)$$

Substituting the component of angular velocity vector $\boldsymbol{\omega}_B^I$ and its derivative $\dot{\boldsymbol{\omega}}_B^I$ into Equation (14) yields

$$\begin{bmatrix} \ddot{\phi} \\ \ddot{\theta} \\ \ddot{\psi} \end{bmatrix} \approx \begin{bmatrix} 4(\kappa - 1)\omega_o^2\phi + \kappa\omega_o\dot{\psi} \\ 3(\kappa - 1)\omega_o^2\theta \\ -\omega_o\dot{\phi} \end{bmatrix} \quad (16)$$

where $\kappa = I_{zz}/I_t$

It can be seen that the pitch is separated from roll and yaw under small rotation angles. There is only a coupling term between roll and yaw.

4. Implemented EKF (sEKF) Estimator

The assumptions of the EKF estimator are listed as follows:

1) The spacecraft is nominally Earth pointing with either a certain spin rate in **Z** axis or 3-axis stabilised.

2) The spacecraft has a symmetric structure on **X** and **Y** axes ($I_{xx} = I_{yy} = I_t$ = transverse inertia momentum), and without any cross terms.

3) The orbit of the spacecraft is near circular with an almost constant angular rate.

4) The system noise model has zero mean.

4.1 State Vector

From Equation (16), it is explicitly shown that pitch is independently separated from roll and yaw. The novel formulation identifies two state vectors that keep the pitch state independent of roll and yaw, and simplifies the general calculation.

The state vectors $\mathbf{x}_1$ and $\mathbf{x}_2$, are defined as

$$\mathbf{x}_1 = \begin{bmatrix} \phi & \psi & \dot{\phi} & \dot{\psi} \end{bmatrix}^T \tag{17}$$

$$\mathbf{x}_2 = \begin{bmatrix} \theta & \dot{\theta} \end{bmatrix}^T \tag{18}$$

4.2 System Model

The non-linear model is defined as [11]

$$\dot{\mathbf{x}} = \mathbf{f}(\mathbf{x},\ t) + \mathbf{w}(t) \tag{19}$$

where $\mathbf{f}(\mathbf{x},t)$ is a non-linear system model,

$\mathbf{w}(t)$ is a zero mean white system noise with covariance matrix $\mathbf{Q}$

The difference between the actual state vector, $\mathbf{x}$, and estimated state vector, $\hat{\mathbf{x}}$, is defined as the state perturbation, $\Delta\mathbf{x}$

$$\Delta\mathbf{x}(t) = \mathbf{x}(t) - \hat{\mathbf{x}}(t) \tag{20}$$

As it is assumed that $\Delta\mathbf{x}$ is small, the system model can be approximately derived from

$$\mathbf{f}(\mathbf{x},\ t) \approx \mathbf{f}(\hat{\mathbf{x}},\ t) + \mathbf{F}\cdot\Delta\mathbf{x} \tag{21}$$

where $\mathbf{F}$ is a linearised system model defined as

$$\mathbf{F} = \left[\frac{\partial \mathbf{f}}{\partial \mathbf{x}}\right]_{\mathbf{x}=\hat{\mathbf{x}}} \tag{22}$$

As we consider only the torque from the Earth's gravitation field and from magnetorquers, then the dynamics equation of the system model is analytically simplified as

$$\dot{\mathbf{x}}_1 = \begin{bmatrix} \dot{\phi} \\ \dot{\psi} \\ \ddot{\phi} \\ \ddot{\psi} \end{bmatrix} = \begin{bmatrix} \dot{\phi} & & & & \\ \dot{\psi} & & & & \\ 4(\kappa-1)\omega_o^2\phi + \kappa\omega_o\dot{\psi} & + & N_{Mx}/I_t & + & w_x \\ -\omega_o\dot{\phi} & + & N_{Mz}/I_z & + & w_z \end{bmatrix} \tag{23}$$

$$\dot{\mathbf{x}}_2 = \begin{bmatrix} \dot{\theta} \\ \ddot{\theta} \end{bmatrix} = \begin{bmatrix} \partial\theta \\ 3(\kappa-1)\omega_o^2\theta & + & N_{My}/I_t & + & w_y \end{bmatrix} \tag{24}$$

Two discrete state transition matrices, Φ_1 and Φ_2, can be approximated for a short sampling period Δt

$$\Phi_1 \approx \mathbf{I}_{4\times4} + \mathbf{F}_1\Delta t \tag{25}$$

$$\Phi_2 \approx \mathbf{I}_{2\times2} + \mathbf{F}_2\Delta t \tag{26}$$

where $\Delta t = t_{(p+1)} - t_{(p)}$.

Therefore, the discrete state perturbation model is then given by

$$\begin{aligned} \Delta\mathbf{x}_{1(p+1)} &= \Phi_{1(p)}\Delta\mathbf{x}_{1(p)} \\ \Delta\mathbf{x}_{2(p+1)} &= \Phi_{2(p)}\Delta\mathbf{x}_{2(p)} \end{aligned} \tag{27}$$

4.3 Measurement Model

A discrete non-linear measurement model is expressed as

$$\mathbf{z} = \mathbf{h}(\mathbf{x},\ t) + \mathbf{m}(t) \tag{28}$$

where $\mathbf{h}(\mathbf{x},t)$ is a non-linear output model,

$\mathbf{m}(t)$ is a zero mean white measurement noise with scalar covariance R.

The linearised innovation error model is given by

$$\begin{aligned}\Delta\mathbf{r}_{(p)} &= \mathbf{z}_{(p)} - \mathbf{h}_{(p)}(\hat{\mathbf{x}},\ t) \\ &= \mathbf{H}_{(p)}\Delta\mathbf{x}_{(p)} + \mathbf{m}_{(p)}(t)\end{aligned} \tag{29}$$

where $\Delta\mathbf{r}_{(p)}$ is an innovation vector at epoch p, an observation matrix $\mathbf{H}_{(p)}$ is defined as

$$\mathbf{H}_{(p)} = \left[\frac{\partial\mathbf{h}_{(p)}}{\partial\mathbf{x}}\right]_{\mathbf{x}=\hat{\mathbf{x}}} \tag{30}$$

The attitude matrix (2-1-3 type) for small angles in roll and pitch, but unlimited yaw rotation is used to calculate the predicted path difference.

$$\hat{\mathbf{A}}_{(p-1)} = \begin{bmatrix} \mathrm{c}\hat{\psi}_{(p-1)} & \mathrm{s}\hat{\psi}_{(p-1)} & \left(-\hat{\theta}_{(p-1)}\mathrm{c}\hat{\psi}_{(p-1)} + \hat{\phi}_{(p-1)}\mathrm{s}\hat{\psi}_{(p-1)}\right) \\ -\mathrm{s}\hat{\psi}_{(p-1)} & \mathrm{c}\hat{\psi}_{(p-1)} & \left(\hat{\theta}_{(p-1)}\mathrm{s}\hat{\psi}_{(p-1)} + \hat{\phi}_{(p-1)}\mathrm{c}\hat{\psi}_{(p-1)}\right) \\ \hat{\theta}_{(p-1)} & -\hat{\phi}_{(p-1)} & 1 \end{bmatrix} \tag{31}$$

At epoch p, an observation matrix for each estimator is then obtained from

$$\mathbf{H}_{1(p)} = \left[\mathbf{b}_B^T\left(\frac{\partial\hat{\mathbf{A}}_{(p-1)}}{\partial\phi}\right)\mathbf{s}_{O(p-1)} \quad \mathbf{b}_B^T\left(\frac{\partial\hat{\mathbf{A}}_{(p-1)}}{\partial\psi}\right)\mathbf{s}_{O(p-1)} \quad 0 \quad 0\right] \tag{32}$$

$$\mathbf{H}_{2(p)} = \left[\mathbf{b}_B^T\left(\frac{\partial\hat{\mathbf{A}}_{(p-1)}}{\partial\theta}\right)\mathbf{s}_{O(p)} \quad 0\right] \tag{33}$$

4.4 Innovation Computation

The innovation is computed as the scalar difference between recovered path difference $\breve{r}$ and predicted path difference $\hat{r}^-$.

$$\delta r = \breve{r} - \hat{r}^- \tag{34}$$

where δr is an innovation for one measurement.

At epoch p, knowledge of the quaternion-attitude, $\hat{\mathbf{A}}$, from the previous epoch (p-1) is required to estimate the predicted path difference, $\hat{r}^-_{(p)}$.

$$\hat{r}^-_{(p)} = \mathbf{b}_B^T\hat{\mathbf{A}}_{(p-1)}\mathbf{s}_{O(p)} \tag{35}$$

For all GPS data at epoch p, the innovation is stacked into a vector $\Delta\mathbf{r}_{(p)}$.

4.5 Covariance Matrices

The error covariance matrices $\mathbf{P}_1$ and $\mathbf{P}_2$, are computed by

$$\mathbf{P}_{1(p)} = \left\langle \Delta\mathbf{x}_1 \cdot \Delta\mathbf{x}_1^T \right\rangle \tag{36}$$

$$\mathbf{P}_{2(p)} = \left\langle \Delta\mathbf{x}_2 \cdot \Delta\mathbf{x}_2^T \right\rangle \tag{37}$$

Note that, two estimators operate simultaneously. The original (6×6) covariance matrix is replaced with the (4×4) $\mathbf{P}_1$ and (2×2) $\mathbf{P}_2$ matrices.

5. Test Results

5.1 Simulated Results

Simulation results presented in this paper are based on a three-axis stabilised satellite in a circular orbit, at 64.5 degrees inclination, and at an altitude of 650 km. The spacecraft orbit was propagated using SGP4 (Simplified General Perturbations 4) orbit propagator [12], which includes geo-gravitational and drag models. The orbits of GPS constellation were propagated using SDP4 (Simplified Deep Perturbations 4). The SDP4 is an extension of SGP4 to be used for deep-space satellites with orbital periods larger than 225 minutes. The lunar-solar perturbations and the effect of resonance caused by non-zonal harmonics for 12 hours are also taken into account of SDP4 model. The nominal simulation parameters are given in Table 1.

Table 1: Nominal Simulation Parameters

parameter	x axis	y axis	z axis
moment of inertia (kg-m^2)	40.0	40.0	40.0
initial attitude (degrees)	0.0	0.0	0.0
initial angular velocity (deg/s)	0.0	-0.06	0.0
baseline coordinates $\mathbf{b}_1$ (mm)	167.7	625.7	0.0
baseline coordinates $\mathbf{b}_2$ (mm)	-625.7	-167.7	0.0

The attitude dynamics based on Equations (5) were implemented to generate the

information of spacecraft orientation. The NORAD (North American Aerospace Defense Command) 2-line elements of TMSAT and operational GPS satellites were used as the initial figures for orbit propagations. The six hours of simulated GPS measurements are used as the input file. It is important to note that in this paper, the measurement error is assumed as white Gaussian with 5 mm rms [3].

The setup parameters for the implemented EKF estimator are shown in Table 2.

Table 2: Setup parameters for EKF estimator

parameter	value	dimension
system noise variance, **Q**	1.0e-6	mixed dimension (rad^2 and rad^2/sec^2)
measurement noise variance, *R*	6.4e-5	$metre^2$
initial guess of attitude angles	0.0	degree
initial guess of angular velocities	0.0	degree/second

Using the EKF estimator, the estimated attitude error (estimated attitude from filtering compared to the true attitude from simulation) in roll, pitch and yaw is plotted in Figure 3, Figure 4 and Figure 5 respectively.

As shown in the simulated results, the attitude error compared to reference solution is less than one degree.

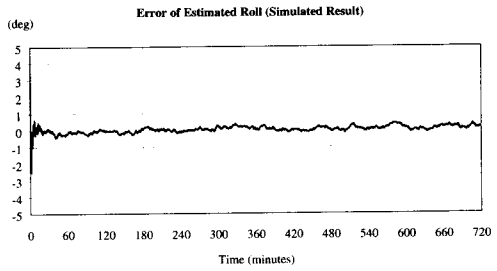

Figure 3. Estimated attitude error in roll

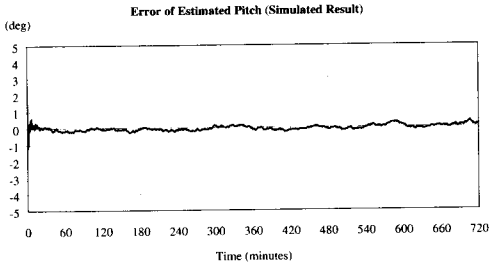

Figure 4. Estimated attitude error in pitch

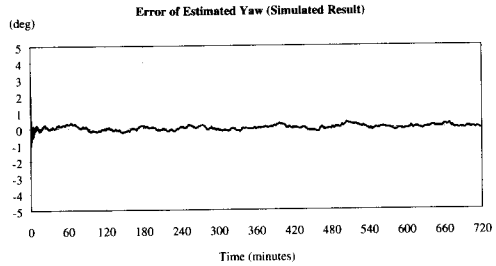

Figure 5. Estimated attitude error in yaw

The estimated angular velocity in Y-axis also closes to the simulated velocity (-0.6 deg/sec) as shown in Figure 6.

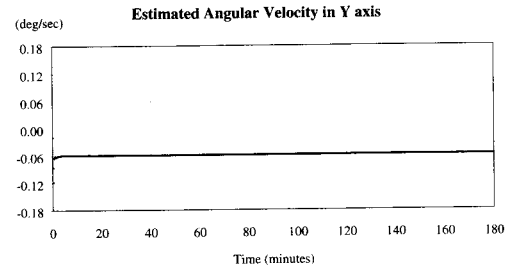

Figure 6. Estimated angular velocity

5.2 Flight Results

This section shows an estimated attitude from real GPS data. A set of phase difference measurements was logged on UoSat-12 minisatellite [13], on 13th January 2000, for 200 minutes.

In January 2000, the UoSat-12 was operated in momentum bias mode. The spacecraft attitude was maintained by magnetic firing and torques generated by a reaction wheel in Y-axis. The logged data of wheel speed

commanded by ADCS (Attitude Determination and Control System) is shown in Figure 7.

The nominal wheel speed was 100 rpm (revolution per minute) approximately. At the 90th minute and 190th minute, spacecraft was commanded to operate under manoeuvre in pitch.

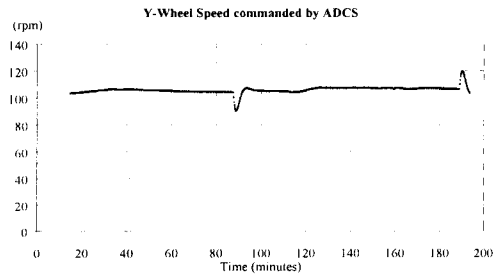

Figure 7. Logged data of Y-wheel speed

The ADCS (Attitude Determination and Control System) attitude on the UoSat-12 was derived from magnetometers and horizon-sensor measurements [14], and used as the reference attitude in evaluating the attitude derived from GPS sensing. The logged data of the computed ADCS attitude is shown in Figure 8.

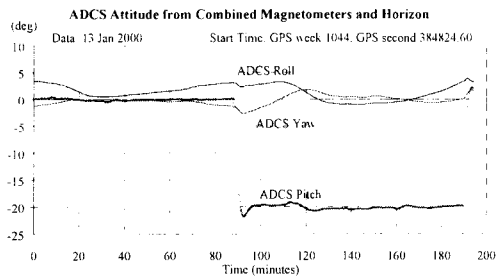

Figure 8. Logged data of UoSat-12 ADCS attitude

Using only GPS data, in acquisition process, a new ambiguity search is performed to estimate and verify initial attitude solution for 5 minutes. A detailed description and results are presented in [13].

In the following process, the EKF estimator is performed to estimate attitude from GPS data collected from two orthogonal antenna-baselines. The initialised elements of R and $\mathbf{Q}$ are the same set that were used in the simulation (given in Table 2).

Figure 9 shows a comparison between the ADCS pitch and GPS pitch estimated from EKF estimator. As can be seen, the estimated attitude using GPS measurements was very close to ADCS attitude. The disparity is less than one degree rms (root mean squares).

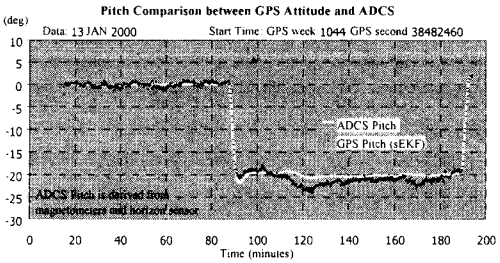

Figure 9. Pitch comparison between ADCS and GPS

The computed one-sigma rms of difference between ADCS attitude and estimated GPS attitude is shown in Table 3.

Table 3: One-sigma rms of difference between GPS attitude and ADCS attitude

disparity in roll	disparity in pitch	disparity in yaw
0.6	0.9°	0.8°

Figure 10 shows an estimated angular velocity in Y-axis using GPS measurements through EKF estimator is very close to the angular velocity computed by ADCS. The rapid changes in angular velocity at 90th minute and 190th minute were caused by the operation of Y-wheel as shown in Figure 10.

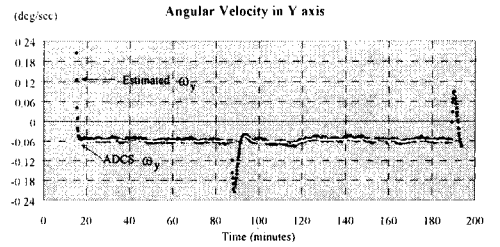

Figure 10. Estimated angular velocity in Y-axis

6. Conclusions and discussions

The Earth-pointing spacecraft dynamics under small rotation angle has been modelled. The analytical formulation has explicitly shown that pitch can be modelled separately from roll and yaw. Therefore, the original state-vector can be split into two state-vectors. Consequently, the two EKF estimators can be processed simultaneously. Furthermore, the maximum dimensions of matrix computation were significantly reduced to (4×4). The attitude estimations from flight GPS data have shown that the implemented EKF estimator provides remarkable results compared to reference ADCS solutions derived from the sophisticated estimator.

Discussions on Kalman Filter are described as follows:

Tuning Kalman filtering:

Generally, the variance of scalar measurement noise R is assumed to be white noise. The value of 6.4e-5 metre (one-sigma = 8.0e-3) was obtained from the calculation of error budget [13].

For UoSat-12, the torque generated by the reaction wheels is considered as the substantial torque with the maximum order of 1.0e-3 Nm. This value was used as the reference for tuning the estimators.

By fixing the R, then the $\mathbf{Q}$ matrix was tuned. The diagonal elements of $\mathbf{Q}$ were set with the value of 1.0e-6 (1 sigma = 1.0e-3). The filtering estimator had performed reasonably well. However, it was found that the attitude solutions started to diverge when the diagonal elements of $\mathbf{Q}$ were lower than 6.4e-7 (1 sigma = 8.0e-4). One explanation is that the filtering estimator tries to follow the attitude dynamics as modelled in the system equation. But, the system model itself cannot cope with the actuator torques. Therefore, the filtering solution starts to diverge when the small value of $\mathbf{Q}$ elements is set. By contrast, with high value of $\mathbf{Q}$ elements, the attitude solution still converged, but has more noise. The explanation was that the filtering estimator has a shorter time constant and tries to follow the measurements rather than attitude dynamic model.

Merits of Kalman Filtering

Using only a few GPS measurements from the number of baselines which can be reduced to one, the Kalman filter can still provide GPS attitude solutions. However, Kalman filters are notoriously dependent on correct initialisation, and if the dynamics models are incorrect, the results may diverge, or provide an inaccurate attitude solution. Another drawback is that the Kalman filter is not so easy to apply for general space applications, as initial attitude manoeuvre must be known, and knowledge of moments of inertia, and torques from actuators are required.

7. Acknowledgement

An author would like to thank Dr.Martin Unwin and Surrey Space Centre for providing worthy flight GPS data.

References

[1] Larson, W.J. and Wertz, J.R., Space Mission Analysis and Design, 3rd Edition, Kluwer Academic Publishers, 2000.

[2]P. Axelrad, and J. Kelley, Near-Earth Orbit Determination and Rendezvous Navigation using GPS, Proceedings of IEEE PLANS, 1986.

[3] Cohen, C.E, Attitude Determination Using GPS, Ph.D. Dissertation, Stanford University, 1992.

[4] Unwin, M.J., The Design and Implementation of a Small Satellite Navigation Unit Based on a Global Positioning System Receiver, Ph.D. Dissertation, University of Surrey, 1995.

[5] Bauer, F.H., Hartman, K., and Lightsey, G.E., Spaceborne GPS Current Status and Future Visions, Proceedings of ION GPS-98, Nashville, TN, September, 1998.

[6] Shuster, M.D., and Oh, S.D., Three-Axis Attitude Determination from Vector Observations, Journal of Guidance and Control, Vol.4, No.1, pp. 70-77, 1981.

[7] Wertz, J.R., Spacecraft Attitude Determination and Control, Kluwer Academic Publishers, 1978.

[8] Kalman, R.E., A New Approach to Linear Filtering and Prediction Problems, J. Basic Eng., Vol. 82D, pp. 35-45, March, 1960.

[9] Lefferts, E.J., Markley, F.L., Shuster, M.D., Kalman Filtering for Spacecraft Attitude Estimation, Journal of Guidance and Control, Vol.5, No.5, 1982.

[10] Fujikawa, S.J. and Zimbelman, D.F., Spacecraft Attitude Determination by Kalman Filtering of Global Positioning System Signals, Journal of Guidance, Control, and Dynamics, Vol. 18, No. 6, November, 1995.

[11] Brown, R.G. Hwang, P.Y.C., Introduction to Random Signals and Applied Kalman Filtering, Third Edition, John Wiley, 1997.

[12] Hoots, F.R. and Roehrich, R.L., Models for Propagation of NORAD Element Sets, Project Spacetrack Report Number 3, Aerospace Defense Center, December, 1980.

[13] Purivigraipong, S., Unwin, M.J., and Hashida, Y., Demonstrating GPS Attitude Determination from UoSat-12 Flight Data, Proceedings of ION GPS-2000, Salt Lake City, UT, September, 2000.

[14] Steyn, W.H. and Hashida, Y., In-Orbit Attitude and Orbit Control Commissioning of UoSat-12, Proceedings of the 4th ESA International Conference on Spacecraft Guidance, Navigation and Control System, ESTEC, Noordwijk, 1999,